REVERSIBILITY OF LIGHT-INDUCED EXCITED SPIN STATE TRAPPING IN THE $Fe(ptz)_6(BF_4)_2$ AND THE $Zn_{1-x}Fe_x(ptz)_6(BF_4)_2$ SPIN-CROSSOVER SYSTEMS

A. HAUSER

Research School of Chemistry, Australian National University, GPO Box 4, Canberra, ACT 2601, Australia

Received 25 November 1985; in final form 3 January 1986

$Fe(ptz)_6(BF_4)_2$ (ptz = 1-propyltetrazole) is an iron(II) spin-crossover system which shows light-induced excited spin state trapping. In this paper we show that (a) the same phenomenon can also be observed in $Zn_{1-x}Fe_x(ptz)_6(BF_4)_2$ ($x \approx 0.1$) and is therefore basically a single-ion property, and (b) that the phenomenon is reversible. The efficiency of the light-induced spin crossover is of the order of 0.5% in the forward direction and 0.1% in the reverse direction.

1. Introduction

Recently Decurtins et al. [1–3] showed that in many iron(II) compounds which exhibit thermal (entropy driven) low-spin (LS) → high-spin (HS) transitions, light-induced LS ($^1A_1$) → HS ($^5T_2$) conversion can be observed by irradiating into the spin-allowed $^1A_1 \rightarrow {}^1T_1$ absorption band at temperatures well below the thermal transition temperature. A mechanism for this phenomenon, subsequently termed "light-induced excited spin state trapping (LIESST)" was proposed [2]. Fig. 1 shows the potential energy surfaces diagram of the low-lying ligand field states for a d^6 system appropriate for a ligand field strength in the region of spin crossover [4]. A schematic representation of the proposed mechanism is indicated: it involves intersystem crossing from the excited $^1T_1$ state to an intermediate low-lying $^3T_1$ state and from there to the $^5T_2$ state where at sufficiently low temperatures the system remains trapped. Inspection of fig. 1 predicts that LIESST should be reversible, i.e. by selectively irradiating into the $^5T_2 \rightarrow {}^5E$ band it should be possible to convert the system back to the $^1A_1$ state. Preliminary experiments confirmed this prediction [2].

$Fe(ptz)_6(BF_4)_2$ (ptz = 1-propyltetrazole), the compound under consideration, shows an extremely sharp thermally induced spin transition around 130 K [5]. It exhibits the normal LIESST effect (trapping of the $^5T_2$ state) below 50 K; above that temperature it relaxes back to the $^1A_1$ state with a strong deviation from first-order kinetics [2]. Both the extremely sharp spin transition and the relaxation from the light-induced $^5T_2$ state indicate that cooperative lattice effects are important.

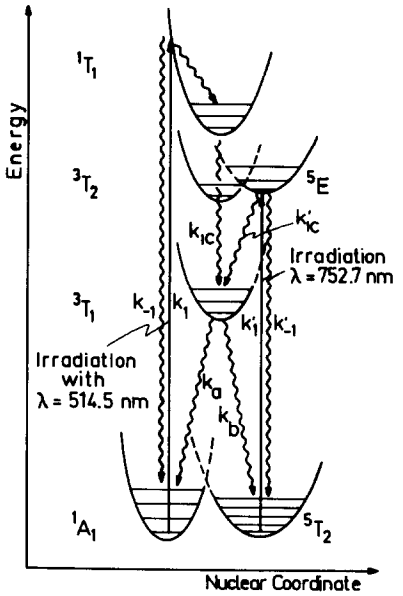

Fig. 1. Schematic potential energy surfaces of the low-lying d^6 ligand field states. Arrows illustrate the mechanism and the reversibility of LIESST.

0 009-2614/86/$ 03.50 © Elsevier Science Publishers B.V.
(North-Holland Physics Publishing Division)

In this paper it is shown that in pure $Fe(ptz)_6(BF_4)_2$ as well as in the doped $Zn_{1-x}Fe_x(ptz)_6(BF_4)_2$ ($x \approx 0.1$) LIESST is indeed reversible. A quantitative analysis of the results shows that in LIESST itself cooperative effects are of little, if any, importance.

2. Experimental

$Fe(ptz)_6(BF_4)_2$ was prepared according to a procedure previously described [5]. Pure $Zn(ptz)_6(BF_4)_2$ was prepared in the same way. Single crystals in the form of colourless hexagonal plates up to several millimeters in diameter of the pure $Fe(ptz)_6(BF_4)_2$ as well as the doped $Zn_{1-x}Fe_x(ptz)_6(BF_4)_2$ were grown from aqueous solutions. A mixture of $Fe(ptz)_6^{2+}$ to $Zn(ptz)_6^{2+}$ of 1 : 4 in solution resulted in crystals with $x \approx 0.1$.

Single-crystal absorption spectra were generated from single-beam transmission spectra recorded with a 3/4 m Czerny–Turner monochromator (Spex 1702) with a grating blazed at 500 nm for light dispersion, a 150 W tungsten lamp as light source, and an EMI 9558 photomultiplier tube (400–800 nm) and a cooled InSb detector (800–1300 nm) for light detection. Sample temperatures down to below 10 K were achieved with an Oxford Instruments SM5 cryostat. For irradiation into the $^1A_1 \rightarrow {}^1T_1$ (ϵ_{max} at 18400 cm^{-1}) and $^5T_2 \rightarrow {}^5E$ (ϵ_{max} at 12250 cm^{-1}) absorption bands the 514.5 nm line of a cw Ar^+ laser and 752.7 nm line of a cw Kr^+ laser (Spectra Physics 164) were used respectively, with laser power levels of 0.35 to 1.1 mW/mm^2 on the sample.

The crystals were irradiated along the hexagonal axis. Due to substantial domain scattering during LIESST it was not possible just to monitor the transmission at the wavelength of the laser line, a transmission spectrum had to be recorded for each time point. The light levels used in recording the spectra can be neglected.

3. Theory

Taking the simple case of a single-ion model for LIESST (i.e. no cooperative effects), it is in principle straightforward to obtain theoretical expressions for the buildup of the HS state (HS fraction γ_{HS}) or the depletion of the LS state (γ_{LS}) as a function of irradiation time. This involves solving the rather complicated set of linear differential equations resulting from the reaction scheme depicted in fig. 1. The only rate constant known a priori is the rate of excitation:

$$k_1 = \tilde{k}_1(\epsilon_\lambda) I_\lambda^0 \qquad (1)$$

(ϵ_λ is the molar extinction coefficient, I_λ^0 is the incident light intensity at wavelength λ), where $\tilde{k}_1$ can be calculated from ϵ_λ [6]. However, already on a qualitative basis we can say that the efficiency of LIESST is fairly low, suggesting that we assume $k_{-1} \gg k_{IC}$. In this case $\gamma_{LS}(t)$ and $\gamma_{HS}(t)$ will show approximately exponential behaviour, namely

$$\gamma_{LS} \approx \gamma_{LS}(0) \exp(-k_{eff} t) ,$$

$$\gamma_{HS} \approx \gamma_{HS}(\infty)[1 - \exp(k_{eff} t)] , \qquad (2)$$

with the effective rate constant k_{eff} being a complicated function of k_1, k_{-1}, k_{IC}, k_a and k_b, and depending upon the input laser power in the same way as k_1, i.e.

$$k_{eff} = \tilde{k}_{eff} I_\lambda^0 . \qquad (3)$$

The efficiency of LIESST can now be defined as

$$\Phi_L = k_{eff}/k_1 = \tilde{k}_{eff}/\tilde{k}_1 , \qquad (4)$$

independent of the input laser power.

A further complication arises from the fact that especially for the pure compound the optical density OD_λ can be fairly high. The light intensity during irradiation will therefore not be constant throughout the crystal and, furthermore, it will vary with time at any given point as the system changes from LS to HS, leading to the following set of coupled differential equations (see insert of fig. 2 for definition of coordinates and symbols):

$$\partial I_\lambda(x, t)/\partial x = -\alpha_\lambda c_{LS}(x, t) I_\lambda(x, t) , \qquad (5a)$$

$$\partial c_{LS}(x, t)/\partial t = -\tilde{k}_{eff} c_{LS}(x, t) I_\lambda(x, t) , \qquad (5b)$$

with $c_{LS}(x, 0) = c^0$, total molar concentration of iron (II), $I_\lambda(0, t) = I_\lambda^0$, incident laser power, $\alpha_\lambda = \epsilon_\lambda \ln(10)$. This system of coupled differential equations is best solved numerically, using a predictor–corrector algorithm. We are basically only interested in $I_\lambda(x_0, t)$ (x_0: thickness of crystal), the observed quantity being

$I_\lambda(x_0, t)/I_\lambda^0$ from transmission spectra. The mean optical density $\overline{OD}_\lambda(t)$ and the mean low-spin fraction $\bar{\gamma}_{LS}(t)$ are related to this quantity in the following way:

$$\bar{\gamma}_{LS}(t) = \frac{\overline{OD}_\lambda(t)}{OD_\lambda(0)} = \frac{\log[I_\lambda^0/I_\lambda(x_0, t)]}{\log[I_\lambda^0/I_\lambda(x_0, 0)]} . \quad (6)$$

For sufficiently thin crystals and especially for the doped material with $OD_\lambda(0) < 0.1$ the variation of I_λ through the crystal is negligible, in which case the numerical solution of (6) becomes identical to the simple exponential behaviour of eq. (2).

4. Results and discussion

In figs. 2 and 3 the absorption spectra at 10 K of $Fe(ptz)_6(BF_4)_2$ and the doped $Zn_{1-x}Fe(ptz)_6(BF_4)_2$ ($x \approx 0.1$) before irradiation, after irradiation at 10 K with the 514.5 nm Ar^+ and subsequent irradiation with the 752.7 nm Kr^+ laser line are shown. The fact that LIESST is observed in the doped as well as in the pure material indicates that it is basically a single-ion phenomenon. The spectra taken after the second irradiation clearly prove that LIESST is reversible, thus supporting our model mechanism with the intersystem crossing to a low-lying intermediate $^3T_1$ state. In the forward LIESST direction $^1A_1 \rightarrow {}^5T_2$ an alternative mechanism with direct crossover from the excited $^1T_1$ to the ^5E state involving higher-order spin–orbit coupling and low-symmetry ligand fields and subsequent non-radiative decay to the $^5T_2$ state cannot be entirely ruled out, since the energies of $^1T_1$ and ^5E as well as that of $^3T_1$ at the equilibrium nuclear configuration of the $^1T_1$ are all fairly close together. However, in the reverse LIESST a direct crossover from ^5E to $^1T_1$ is out of the question for energetic reasons and the presence of the low-lying triplet states acting as intermediates is essential.

For a quantitative treatment of LIESST let us first concentrate on the forward direction $^1A_1 \rightarrow {}^5T_2$. In fig. 4a the mean low-spin fraction $\bar{\gamma}_{LS}$ as a function of time or rather as a function of integrated laser power at 514.5 nm for two pure crystals of different thickness and one doped crystal are shown. All three curves

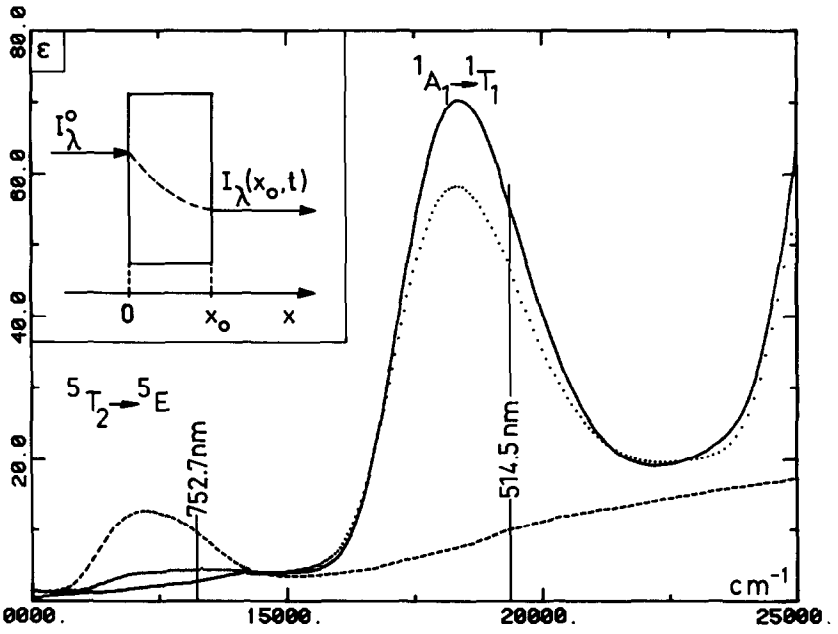

Fig. 2. Near-infrared and visible absorption spectra of $Fe(ptz)_6(BF_4)_2$ at 10 K : (—) normal spectrum, (– – –) after irradiation with λ = 514.5 nm (≈300 mJ), (•••) after subsequent irradiation with λ = 752.7 nm (≈3000 mJ). Insert : apparatus for irradiation (x parallel to trigonal crystal axis, x_0 is thickness of crystal, I_λ^0 is intensity of incident laser beam).

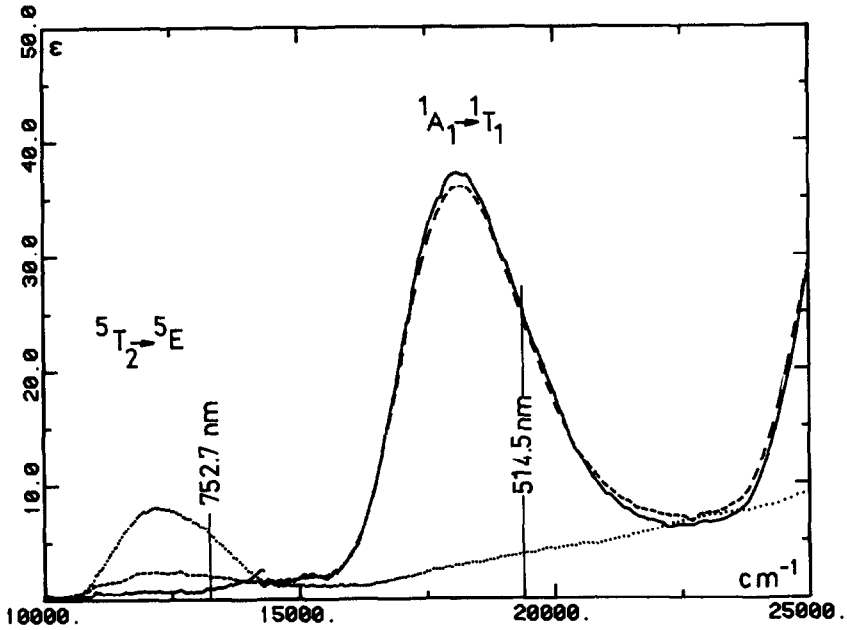

Fig. 3. Absorption spectra of $Zn_{1-x}Fe_x(ptz)_6(BF_4)_2$ ($x \approx 0.1$) at 10 K : (——) normal spectrum, (•••) after irradiation with λ = 514.5 nm, (– – –) after subsequent irradiation with λ = 752.7 nm.

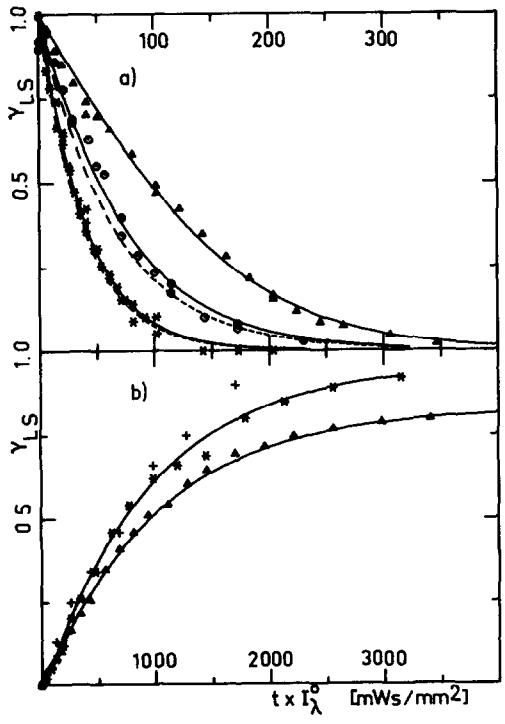

were fitted with a least-squares fitting routine to the solution of the differential equations (5a) and (5b). For the actual fitting procedure however, not the $\bar{\gamma}_{LS}(t)$ curves of fig. 4a were used, but the original $I_\lambda(x_0, t)/I_\lambda^0$ curves, as determined from the transmission spectra with $\tau = \tilde{k}_{eff} I_\lambda^0$ and $\xi = \alpha_\lambda c^0 x_0$ as free parameters. $\tilde{k}_{eff}$ can easily be calculated if I_λ^0 is known, and using eq. (6) $\bar{\gamma}_{LS}(t)$ follows directly. The second parameter immediately yields ϵ_λ provided c^0 and x_0 are known. The fits are quite satisfactory and the resulting parameters are listed in table 1 (a). For comparison the exponential decay curves calculated using the respective rate constants for the pure and the doped material are included in fig. 4a. It is clear that the thin-

◀ Fig. 4. (a) LIESST kinetics: γ_{LS} as a function of irradiation energy with λ = 514.5 nm. (⊙) $Fe(ptz)_6(BF_4)_2$ crystal No. 1, (△) crystal No. 2, (*) $Zn_{1-x}Fe_x(ptz)_6(BF_4)_2$ crystal No. 1; (——) calculated curves according to eq. (5), using parameters of table 1 (a) (– – –) calculated exponential decay using the same parameters. (b) Reverse LIESST kinetics: γ_{LS} as a function of irradiation energy with λ = 752.7 nm. (*, +) $Zn_{1-x}Fe_x(ptz)_6(BF_4)_2$ crystal No. 2, (△) $Fe(ptz)_6(BF_4)_2$ crystal No. 3; (——) exponential fits according to eq. (2).

Table 1
Parameters relevant to the kinetics of LIESST in the forward and reverse direction for $Fe(ptz)_6(BF_4)_2$ and Zn : Fe(12%) $(ptz)_6(BF_4)_2$. x_0 is thickness of crystal, OD_λ and ϵ_λ are optical density and extinction coefficient at the wavelength of irradiation, $\xi = \alpha_\lambda c^0 x_0$, $\tilde{k}_{eff}$ rate of light-induced spin crossover, $\tilde{k}_1$ rate of excitation, Φ_L and Φ_R efficiency of LIESST in the forward and reverse directions respectively

	(a) LIESST						
	$x_0(\mu m)$	$OD_{514.5}$	ξ	$\tilde{k}_{eff}(mm^2/mW\,s)$	$\epsilon_{514.5}$	$\tilde{k}_1(mm^2/mW\,s)$	$\Phi_L(\%)$
$Fe(ptz)_6(BF_4)_2$							
crystal No. 1	31	0.21	0.48(2)	$1.54(8) \times 10^{-2}$	44	3.1	≈0.5
crystal No. 2	155	0.89	2.06(3)	$1.40(4) \times 10^{-2}$			
Zn : Fe(12%) $(ptz)_6(BF_4)_2$							
crystal No. 1	–	0.12	0.18(1)	$2.60(5) \times 10^{-2}$	23	1.6	≈1.5
	(b) reverse LIESST						
	$x_0(\mu m)$	$OD_{752.7}$	$\gamma_{LS}(\infty)$	$\tilde{k}'_{eff}(mm^2/mW\,s)$	$\epsilon_{752.7}$	$\tilde{k}'_1(mm^2/mW\,s)$	$\Phi_R(\%)$
$Fe(ptz)_6(BF_4)_2$							
crystal No. 3	–	0.05	0.85(2)	$1.00(5) \times 10^{-3}$	9.2	0.93	≈0.1
Zn : Fe(12%) $(ptz)_6(BF_4)_2$							
crystal No. 2	275	0.022	0.99(2)	$1.06(9) \times 10^{-3}$	4.8	0.49	≈0.2

ner the crystal and therefore the smaller $OD_\lambda(0)$ the closer $\bar{\gamma}_{LS}(t)$ is to the exponential curve.

Taking $\tilde{k}_1$ calculated from ϵ_λ according to [6] from table 1 (a) the efficiency Φ_L of LIESST is estimated to be ≈0.5% for the pure and slightly higher for the doped material.

Exactly the same procedure can be followed for the reverse LIESST, irradiating into the $^5T_2 \rightarrow {}^5E$ band of the trapped species. As ϵ_λ at $\lambda = 752.7$ nm is much lower than at 514.5 nm and only a comparatively thin crystal was used in the case of the pure compound, $OD_\lambda(0) < 0.1$ was satisfied and equations (2) could be applied (in this case with "LS" and "HS" exchanged). The results of a least-squares fit, using $\tilde{k}'_{eff} I^0_\lambda$ and $\gamma_{LS}(\infty)$ as variable parameters, are listed in table 1 (b). In fig. 4b the experimental and calculated $\gamma_{LS}(t)$ curves are shown. $\tilde{k}'_{eff}$ seems to be much smaller for the reverse LIESST, but since $\epsilon_{752.7} < \epsilon_{514.5}$ the excitation rate $\tilde{k}'_1$ is also lower, and the efficiency $\Phi_R = \tilde{k}'_{eff}/k'_1$ is with ≈ 0.1% of the same order of magnitude as for the forward direction. A further point to note is that in the doped material LIESST is 100% reversible, whereas in the pure compound $\gamma_{LS}(\infty) = 0.85$. This could be due to large internal strain as the difference in metal-to-ligand bond-length between the HS and the LS state is 0.1–0.2 Å [7].

5. Conclusions

We have shown that LIESST is basically a single-ion phenomenon, since it is observed in the doped as well as in the pure compound. In contrast to the thermal spin crossover and the HS → LS relaxation [2], it is not much influenced by any cooperative lattice effects. In principle LIESST is fully reversible. The efficiencies of LIESST in the forward and reverse directions are of the same order of magnitude, the former being somewhat larger. It is unfortunately not possible to determine the intersystem crossing rates k_{IC} and k'_{IC} and the partitioning rates k_a and k_b individually. The fact that LIESST is reversible, however, indicates that k_a and k_b are of the same order of magnitude and that the intersystem crossing rates determine the order of magnitude of the efficiency of LIESST.

In systems which show thermal spin crossover, the minimum of the $^1A_1$ potential well lies typically 500 cm^{-1} below that of the $^5T_2$ [7]. It should now be possible to find a system in which this difference is smaller or even with the $^5T_2$ slightly below the $^1A_1$. Such a system would be HS down to very low temperatures, but it should be possible to trap the $^1A_1$ state by irradiating into $^5T_2 \rightarrow {}^5E$ band at low temperatures

in much the same way as in our present system the $^5T_2$ state can be trapped.

Acknowledgement

I thank M. Puza for the preparation of the compounds used in this work.

References

[1] S. Decurtins, P. Gütlich, C.P. Köhler, H. Spiering and A. Hauser, Chem. Phys. Letters 105 (1984) 1.
[2] S. Decurtins, P. Gütlich, K.M. Hasselbach, A. Hauser and H. Spiering, Inorg. Chem. 24 (1985) 2174.
[3] S. Decurtins, P. Gütlich, C.P. Köhler and H. Spiering, J. Chem. Soc. Chem. Commun. (1985) 430.
[4] S. Sugano, Y. Tanabe and H. Kamimura, Multiplets of transition metal ions (Academic Press, New York, 1970) p. 110.
[5] P.L. Franke, J.G. Haasford and A.P. Zuur, Inorg. Chim. Acta 59 (1982) 5.
[6] J.B. Birks, Photophysics of aromatic molecules (Wiley–Interscience, New York, 1970) p. 44.
[7] P. Gütlich, Struct. Bonding 44 (1981) 140.